



School of Physics and Astronomy
University of Birmingham
Edgbaston
Birmingham
B15 2TT



Forschung mit Lepton Collidern (FLC) Group
Deutsches Elektronen-Synchrotron (DESY)
Notkestraße 85
D-22607
Hamburg

The Characterisation of Silicon Strip Sensors as an external tracker for the Large Prototype Time Projection Chamber at the Deutsches Elektronen-Synchrotron.

Dwayne SPITERI

September 8, 2015

Main Supervisor: Dr Dimitra Tsionou and Dr Ties Behnke
Assistant Supervisors: Dr Annika Vauth and Aliakbar Emrahimi

Word Count: 3911

1 Abstract

In this report, the electrical characteristics of three silicon sensors; SILC08, SILC10 (CMS) and SILC11, are explored. All the sensors showed no voltage breakdown up to 700V, with SILC08 and SILC11 showing no breakdown up to 800V. SILC08 and SILC11 had a depletion voltage of 50-60V, whereas the CMS sensor had a measured depletion voltage of 300V. All the sensors had a current leakage of 2 orders of magnitude lower than the bias current at low voltages, but at high voltages the SILC08 sensor had a current leakage of the same order of magnitude as the bias current. The resistances of the bias resistors on the SILC11 and SILC08 sensors seem to be consistent with a resistance of about 30M Ω , and the CMS sensor measurements are consistent with a resistance of $2.0 \pm 0.6 \text{M}\Omega$.

Contents

1	Abstract	1
2	Introduction	2
3	Background	2
3.1	The ILC	2
3.2	The ILD Tracker	3
3.3	The LPTPC	3
3.4	The LPTPC External Tracker	4
4	Silicon Sensors	5
4.1	The General Principle of Silicon Semiconductor Sensors	5
4.2	Strip Sensors	6
4.2.1	The SILC Sensors	6
5	Apparatus and Methodology	7
5.1	The Experimental Set-up	7
5.2	IV-CV Setup	9
5.2.1	The IV Set-up	9
5.2.2	The CV Set-up	9
5.3	Resistances Setup	10
5.3.1	Bias Resistance	10
5.3.2	Inter-strip measurements	10
6	Results and Analysis	11
6.1	Breakdown Voltages from IV Curves	11
6.2	Current Leakage from IV Curves	11
6.3	Depletion Voltages from CV Curves	13
6.4	Bias Resistances	13
7	Conclusion and Outlook	15
8	References	17
9	Acknowledgements	17

2 Introduction

The main aim of this study was to measure and compare the electric characteristics of two sensors obtained from the SIL collaboration (or SILC); SILC08 and SILC11 and a CMS test sensor (SILC10). These characteristics are obtained by performing a series of current, voltage and capacitance measurements on these sensors at a manual probe-station. The goal is that these sensors could be used as an external tracker for the Large Prototype Time Projection Chamber (LPTPC) at DESY. This report will give a short introduction as to the origin of the motivation behind such measurements, followed by an outline of the technology, and then lead into analysis of the data taken from the sensors.

3 Background

This section will give a brief introduction to the ILC experiment and the LPTPC. It will also discuss why silicon sensors are needed in the LPTPC and how they will be incorporated into the final design.

3.1 The ILC

The International Linear Collider (ILC), pictured below in figure 1, is a future collider concept designed to collide electrons and positrons at centre of mass energies of 500GeV, but will become 1TeV with later upgrades. The LHC mainly aims to study precision physics and it's efforts will be complimentary to the LHC Run II. The ILC concept includes two detectors: the International Large Detector (ILD) and the Silicon Detector (SiD) operated based on a 'push-pull' scheme around the interaction point[1]. Currently research and development is undergoing into optimising the detectors construction such that the design requirements for the detectors can be met. This document will focus on research for the ILD tracker.

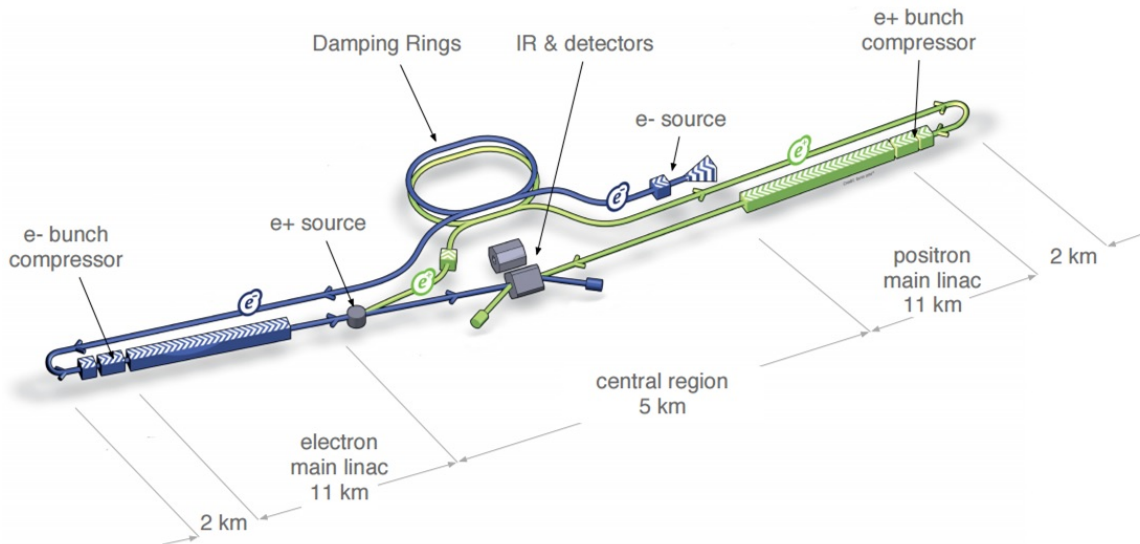


Figure 1: A schematic diagram of the ILC with the main subsystems.[1, p9]

3.2 The ILD Tracker

The ILD tracker will consist of a vertex pixel detector (VTX), internal and external Silicon Trackers (SIT, SET), a Time Projection Chamber (TPC) and a forward Silicon tracking detector (FTD). A model of this can be seen in figure 2. One of the groups working on Research and Development for the tracker is the Forschung mit Lepton Colliden Time Projection Chamber (FLC TPC) Group based at DESY.

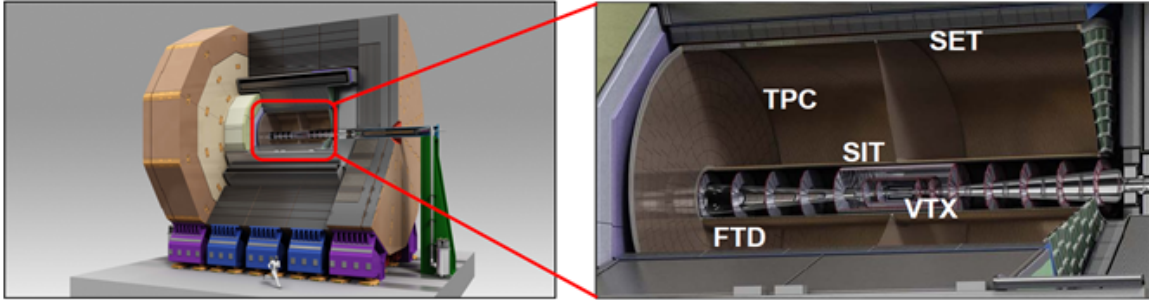


Figure 2: A computer generated design of the ILD and a closer view of the tracking system. [2]

A TPC is a gas detector that can precisely track the trajectory of a charged particle. A charged particle that passes through a TPC will ionise the gas present in its trajectory creating electrons and ions. The several thousand volt potential difference applied across the electrodes will then cause the separated charges to drift to a particular electrode. Readout electronics at the electrodes will multiply the electron signals, and the time difference between each of the electron hits allow the ionisation track to be reconstructed. A magnetic field is also applied parallel to the electric field to bend the trajectory of the initial particle and cause a curve in the reconstructed track. This will allow the charge and momentum of the particle to be measured. The ILD TPC has a momentum resolution requirement of $2 \times 10^{-5} \text{GeV}^{-1}$ [1].

3.3 The LPTPC

The FLC TPC group have built a Large Prototype Time Projection Chamber (LPTPC) at DESY. It has a diameter of 72cm and a length of 61cm, and the test-beam area where it is housed has a 1T magnet structure for the TPC to fit inside. Figure 3 shows a projection of the LPTPC. The main motivation of doing so was to scale up from the individual and very bespoke module testing arrays to a size that could test different readout technologies in a standardised fashion. Scaling up also produced some challenges that needed to be overcome such as the minimisation of the radial thickness (material budget) of the field cage and readout electronics for a prototype of that size [3, p40-42]. The LPTPC is then the first step to the full scale TPC and starts to incorporate a structure that can be replicated and scaled up to the actual size of the ILD TPC.

Currently the TPC has a momentum resolution of $4 \times 10^{-3} \text{GeV}^{-1}$. This is calculated by putting the measured transverse momentum resolution ($\sigma_{r\phi}(x)$) for the TPC of $100 \mu\text{m}$, which is the same as the ILD [4], into the Gluckstern formula for momentum resolution given by equation 1.

$$\frac{\sigma(p_t)}{p_t^2} = \frac{\sigma_{r\phi}(x)}{0.3BL^2} \sqrt{\frac{720}{N+5}} [5], \quad (1)$$

where N is the number of points taken along the track, B is the magnetic field and L is the measurement volume. The LPTPC values for B and L are 1T and 1.5m respectively.

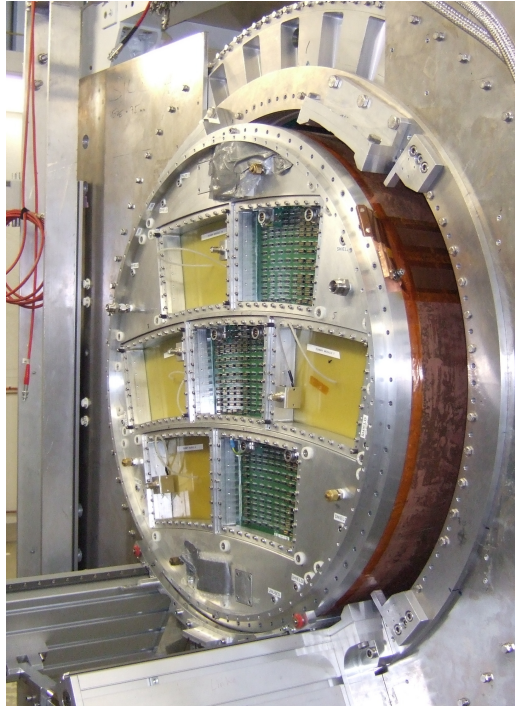


Figure 3: Image of the LPTPC prototype.

3.4 The LPTPC External Tracker

As mentioned above, the Electric and Magnetic fields in the TPC are parallel to each other, which allows the secondary electrons to move to the anode unaffected by the magnetic fields. However, along the TPC, and in particular close to the module edges the E-field can lines can bend and this can cause distortion ($E \wedge B$) effects. In order to understand and correct for these effects, an external detector is required in order to provide reference tracks.

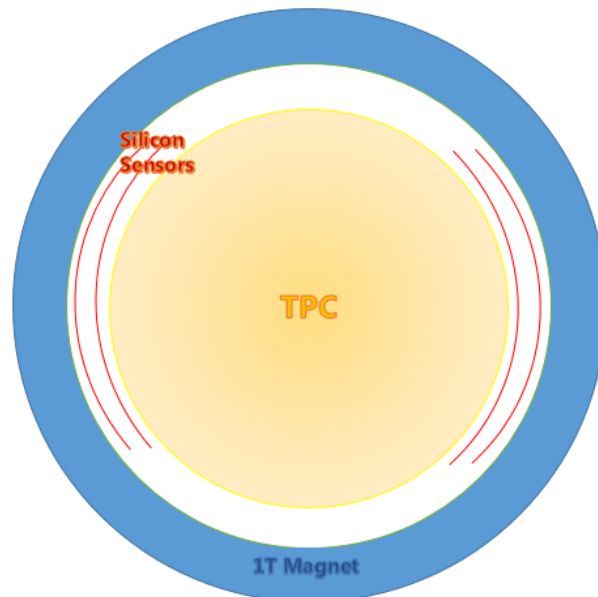


Figure 4: Schematic diagram of how the external tracker will fit in the current set-up.

Like the planned ILD TPC, the external tracker for the LPTPC will be made from semicon-

ductor silicon sensors. Figure 4 shows a not-to-scale schematic of how the external tracker will be incorporated into the existing structure of the LPTPC. Since the external tracker will be required to give an independent measurement of the particle track, it needs a momentum resolution better than, or at the very least equal to, that of the TPC. Section 4.1 will discuss how silicon sensors work in more detail.

Figure 4 depicts four silicon sensors inside the magnet. An internal study[6] showed that this is the optimum number. If there were only two sensors, a helical track could not be fitted; with three sensors, the performance is severely degraded; and with five or more sensors the additional cost of the sensor did not justify the increase in the resolution. The sensors have to be placed inside the inner radius of the magnet in order to obtain the most accurate reference points. Since the set-up has to be oriented this way, another challenge is presented, as the space between the magnet and the TPC is only 3.5cm. Another conclusion of the study, given the limited space for the sensors, was that sensors with a spacial resolution better than $10\mu\text{m}$ are needed to obtain the required resolution. (more about this in section 4.2).

4 Silicon Sensors

This section gives a brief introduction on how semiconductor silicon detectors work, a description of the SILC sensors used, and gives an outline of the key features for the SILC sensors.

4.1 The General Principle of Silicon Semiconductor Sensors

In a planar metallic crystal an atom has 4 neighbours that it can exchange electrons with. Silicon is a valence-4 element which covalently bonds with it's 4 neighbours to form atoms that have full outer shells of electrons. Hence the material has no excess of 'free' electrons or holes. to increase the number of charge carriers the Silicon is doped with a valence-3 material, such that one of the neighbouring Si atoms does not have a full outer shell, creating a hole. This hole acts as a positive charge carrier and is free to migrate through the material. This is called a p-type semiconductor. Conversely when a valence-5 element is doped across a valence-4 metallic crystal, an excess of electrons are created that are free to move around, and an n-type semiconductor is formed.

When an n-type and a p-type are combined, a carrier-free region called a depletion region is formed in the middle where the excess electrons and holes form electron-hole pairs. Since this is the active region of the detector, a voltage difference, called the (reverse) bias voltage, is applied across ends of the detector to extend this region as much as possible.

When a charged particle passes through with the depletion region it gives the electron-hole pairs enough energy to separate, and the charge can be collected by accelerating it towards the respective electrode due to the potential difference applied by the bias voltage. Usually, in high energy physics, the n-type conductor is the material bulk, and the p-type conductors are the strips that lie on the surface of the bulk[7, p13].

For the signal from the accumulated charge to be extracted (for example: through a read-out process), an electrical contact with the silicon is needed. Usually this is in the form of some conducting material like aluminium placed either on the strip (DC pad) or via an intermediate SiO_2 layer (AC pad)[7, p14]. Then the conducting material is connected to a charge sensitive amplifier and other electronics which converts the charge into an output signal.

4.2 Strip Sensors

In a strip sensor the p-type semiconductors are thin strips of either n- or p- doped Silicon. A schematic diagram for a silicon strip sensor is displayed in figure 5.

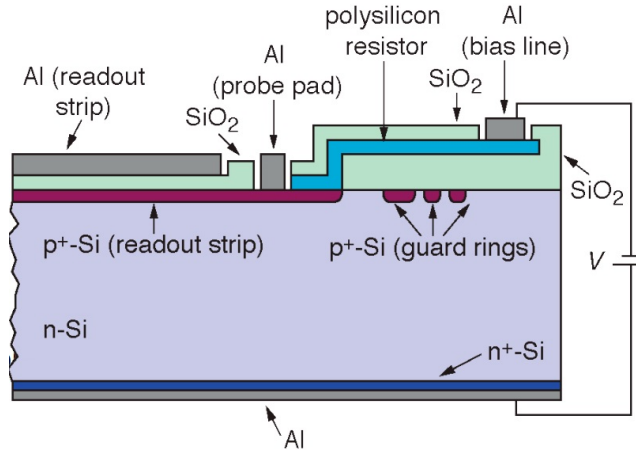


Figure 5: Cross-section of a Polysilicon biased Silicon Sensor[8, p5].

To apply the bias voltage across all the strips equally, a polysilicon bias resistance is used to connect the silicon strip to a bias ring. The advantage of using polysilicon resistors is that they are radiation hard and give linear trends with depletion voltage and bias voltage applied [7, 9]. Other biasing methods exist, such as FOXTET biasing and punch-through biasing, but the former is not radiation hard, and both give non-linear trends for bias voltage to depletion region expansion, and hence are more difficult to operate[7, 9]. The separation between strips is called the strip pitch, d , and is related to the spacial resolution of the sensor by a factor of $\frac{1}{\sqrt{12}}$ [7, p20]. This assumes that a particles track would be confined to a single strip. By using an analogue readout, the spacial resolution can be further improved by using the information from the neighbouring strips when a signal is generated, as the charge generated from a passing particle is usually shared between strips[10].

4.2.1 The SILC Sensors

Three silicon strip sensors were sent to DESY from Vienna. The sensors were named, AIDA-SILC-08 from ILC-AC-SSSD (SILC08), AIDA-SILC-10 from CMS-ST-OBI(SILC10) and AIDA-SILC-11 from ILC-AC-SSSD (SILC11). The sensor SILC10 is a CMS strip sensor that has 768 strips and has a pitch of $120\mu\text{m}$. The resolution is not good enough for an ILD external tracker but it will still be used here for testing purposes. For the duration of the document SILC10 shall be referred to as the CMS sensor. SILC08 and SILC11 have 1792 strips with a $50\mu\text{m}$ pitch which may obtain a final spacial resolution of about $9\mu\text{m}$. Figure 6 shows a photo of one of the sensors under a microscope.

Since the SILC sensors have the correct geometry to suit the need of the LPTPC, it is necessary to test the electrical characteristics of the sensor. Such measurements will also allow the definition of the operation points of the sensor. In particular: the depletion voltage, the breakdown voltage, current leakage versus voltage, the resistance of the bias resistors (called the bias resistance), and the inter-strip resistance can be measured.

The experimental set-up to do this is described in section 5. This is the set-up that will be used to probe all these characteristics via CV-IV measurements and resistance measurements.

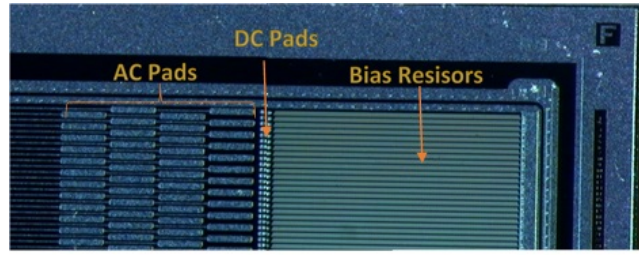


Figure 6: Photo of SILC08 under the microscope. The Bias resistors are 2mm long, the DC pads are $62\mu\text{m}$ long, and the AC pads are $360\mu\text{m}$ long,

5 Apparatus and Methodology

This section will introduce the experimental equipment used, why it is used, and how the relevant characteristics will be probed using it. It also discusses how the relevant parameters can be extracted from the data plots.

5.1 The Experimental Set-up

Figure 7 shows the experimental set-up and equipments while figure 8 shows the inside of the probe-station.

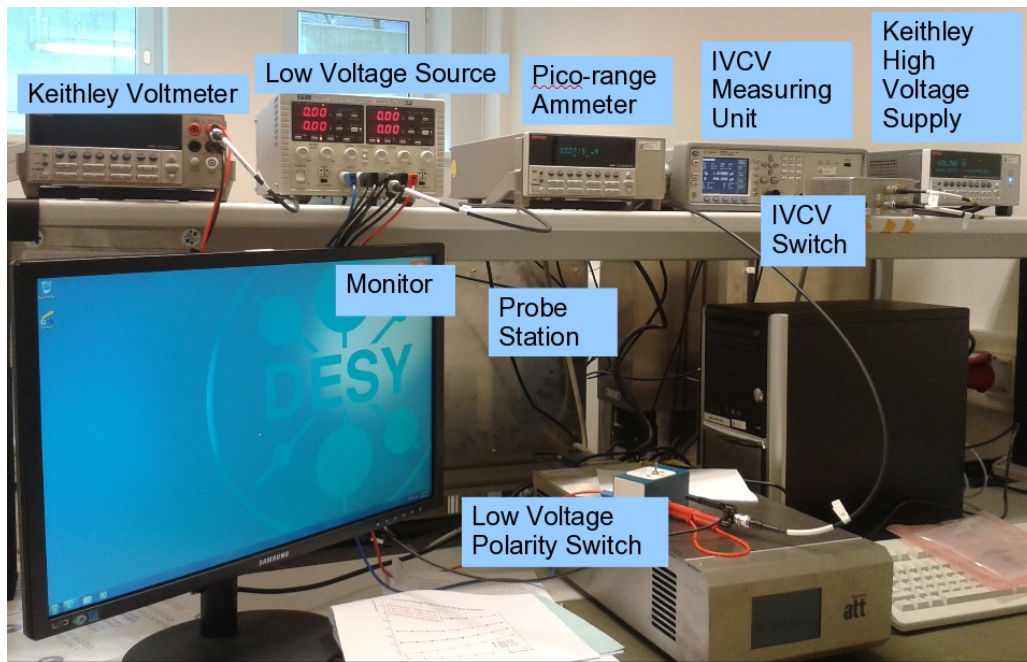


Figure 7: Photo of the experimental set-up with the main electronics labelled.

Keithley High Voltage (HV) Supply

This is used to apply the bias voltage on to the backplane of the sensor. It has two modes. A scanning mode that varies the voltage applied, and a static mode that applies the voltage that is set.

IVCV Measuring unit (LCR Meter)

This is the unit that measures both the capacitance and the current flowing through the

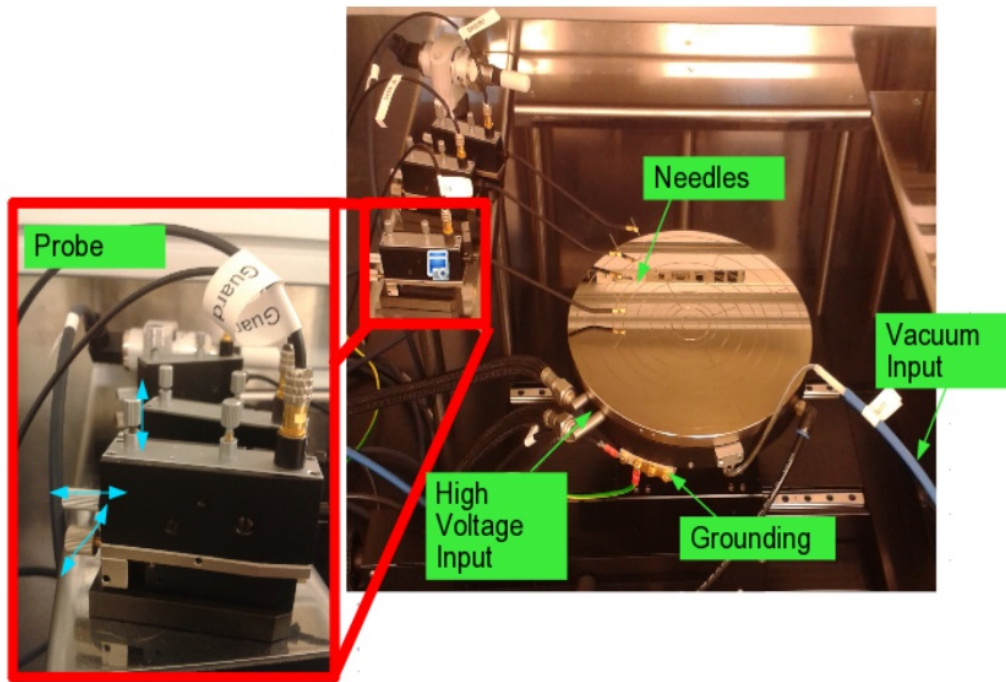


Figure 8: Labelled photo of the inside of the probe station.

ring that the probe connected to this is placed on. It is connected to a PC where this is read by the **XXXXXXXXXXXXXXXXXXXXXXXXXXXX** program.

IVCV Switch

This switches the internal electronics such that IV and CV measurements can be taken with the same device.

Keithley Pico-range Ammeter

This is a high-precision ammeter that will be used to measure current.

Low Voltage Source

This unit is able to apply a voltage difference of up to $\pm 20\text{V}$. It contains two separate voltage units.

Low Voltage Polarity Switch

The switch allows the low voltage source to switch from positive to negative polarity without using another source.

Monitor/PC

The PC will store the data from the IVCV Measuring unit on a programme called **NOBODYKNOWS** and output a .txt file with the measurements for analysis of the data in ROOT.

Probe Station

The sensor to be tested is placed on the circular table and held in place with a vacuum pump. The High Voltage input will be applied to the table which will then be coupled to the back of the sensor. The needles which come into contact with various parts of the sensor are attached to probes that can be finely altered in the three spacial dimensions.

5.2 IV-CV Setup

In order to determine the breakdown and depletion voltages, and the current leakage as a function of applied voltage, a set-up needs to be designed that can perform Current-Voltage (IV) and Capacitance-Voltage (CV) measurements on the sensor.

5.2.1 The IV Set-up

Two probes are placed on the bias ring to obtain the current versus voltage behaviour of the sensor: one is connected to the pico-ammeter, and the other is connected to the IVCV measuring unit (LCR meter). The pico-ammeter output is fed into the LCR meter. The High voltage supply is put on the variable mode and varied from 1V to 700/800V in steps of 5V obtaining 140/160 points. This measures the current flowing through the sensor, which behaves like a diode. Since the sensor is reversely biased, the current reading is expected to increase linearly from the origin, until it reaches the breakdown voltage where it increases dramatically[11, p44]. Figure 9 shows where the probes will be placed and what electronics are used in relation to the sensor.

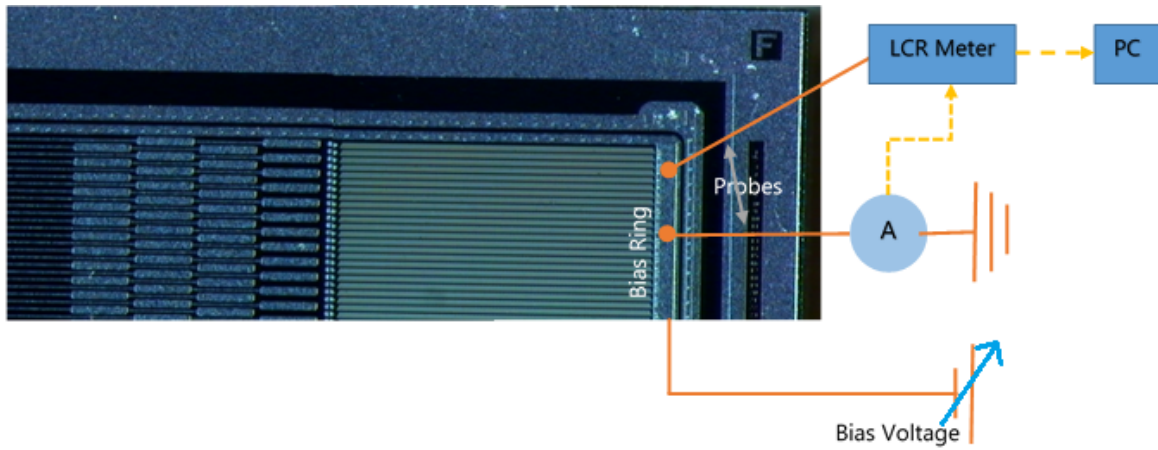


Figure 9: IV measurement set-up on the SILC sensor.

For a measurement of the current leakage versus voltage the ammeter probe is moved to the guard ring. The curve is expected to have the same shape but the current readings should be a few orders of magnitude smaller.

The data output for these measurements will be ordered in columns in a text file. This text file is read in to a ROOT C++ macro and will produce a plot of current against voltage, where it will be analysed for the sharp breakdown voltage increase, or for the comparison of the bias and guard currents.

5.2.2 The CV Set-up

The set-up for the capacitance as a function of voltage measurements is the same as for the IV one with the exception that the IVCV switch is in the CV position.

The data output from **THE PROGRAMME** for the CV measurement contains the capacitance and voltage measurement values. To obtain a value for the depletion region, $\frac{1}{C^2}$ is plotted against V . This will obtain a linear increase which eventually plateaus. The depletion region is then the value of the voltage at the intersection point of the plateau line and the linear increase[12, p110].

5.3 Resistances Setup

In order to measure the bias and inter-strip resistances, a set-up needs to be designed that can perform high-accuracy voltage measurements on the sensor.

5.3.1 Bias Resistance

Again two probes are placed on the bias ring, this time one is connected to the ammeter, and the other is connected the ground. A third probe is connected via the polarity switch to a low voltage power supply. The high voltage supply is kept constant and at a value that fully depletes the sensor. The set-up depicted on the sensor is shown in figure 10. The set-up measures the current flowing through the strip to the ground, and therefore the current that flows through the bias resistor. The low voltage supply will be varied in steps of 2V (1V) and range from -10V to 10V (-5V to 5V) obtaining 11 points.

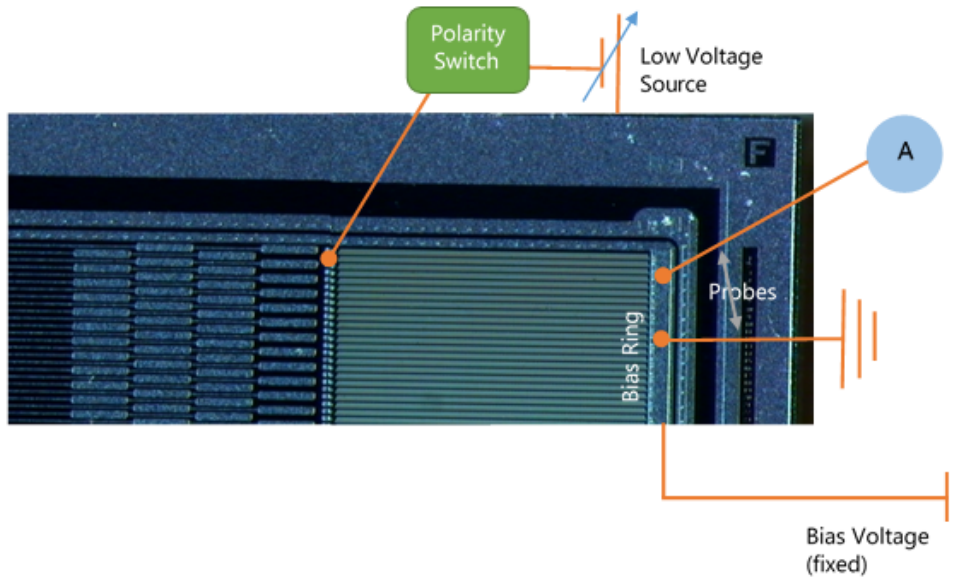


Figure 10: Bias resistance set-up on an image of a SILC sensor.

The current reading is expected to start from a negative value, and increase linearly whilst going through the origin if the resistor is ohmic[11, p4]. Since there is no computer readout for the low-voltage supply or the ammeter, the current and voltage values are taken manually. The data is fed in to a C++ macro in the ROOT framework, which plots the data, following Ohm's Law, to a linear fit. The inverse of the gradient of the fit corresponds to the bias resistance which is expected to be in the order of $M\Omega$'s. The errors on these values are obtained from the variation on the current and voltage measurements as well as the errors from a straight line fit [13, p100].

5.3.2 Inter-strip measurements

The set-up for the inter-strip measurements as a function of low voltage measurements is the same as for the bias resistance with the exception that the current probe on the bias ring is moved to the DC pad on the strip adjacent to the one with the low voltage source on it. This set-up is depicted in figure 11. The current readings are expected to follow the same pattern as the bias resistances with the exception that the expected resistances are in the order of $G\Omega$'s

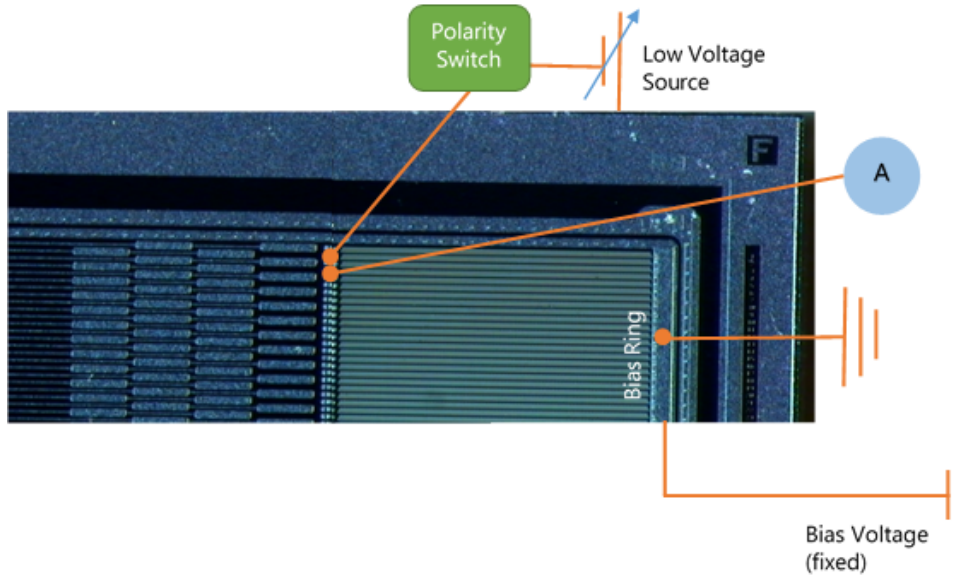


Figure 11: Inter-strip resistance set-up on an image of a SILC sensor.

6 Results and Analysis

This section shows the results of the measurements performed using the set up outlined in the previous section. It explains the result obtained and any developments in the optimisation of the set-up.

6.1 Breakdown Voltages from IV Curves

Figure 12 shows the plot of the bias current as a function of the applied voltage.

Figure 12 shows that for low values of bias voltage, the SILC sensors exhibit the expected behaviour of a diode trend in the linear increasing phase. At higher voltages, the SILC08 sensor exhibits some large current fluctuations. This could be due to a bad connection between the probe and the bias ring. Since the current values do not increase at an exponential rate in this region, it can be said that both of the SILC sensors do not undergo a breakdown at voltages lower than 800V.

The blue line shows the trend for the CMS sensor. The dramatic increase in the current values at around 200V is known as a soft breakdown which occurs as a result of a micro-discharge localised to a single strip[14, p37] and happens before the breakdown voltage. Since the line follows that of the SILC sensor after this soft breakdown, it can also be concluded that the CMS sensor does not breakdown at voltages lower than 700V.

6.2 Current Leakage from IV Curves

Figure 13 shows the plot of the guard current as a function of the applied voltage.

This measurement determines how effective the sensor is at minimising current leakage. The larger the current detected in the guard ring in proportion to the current measured in the bias ring, the less effective the system is at containing the currents generated. In the typical operating region highlighted in light orange in figure 13 the measured current leakage is always two orders of magnitude lower than the bias current (proportion of current leakage of ≈ 0.01). At the largest voltages scanned, the proportion of current leakage for the SILC08 and SILC11 sensors are ≈ 1 and ≈ 0.1 respectively.

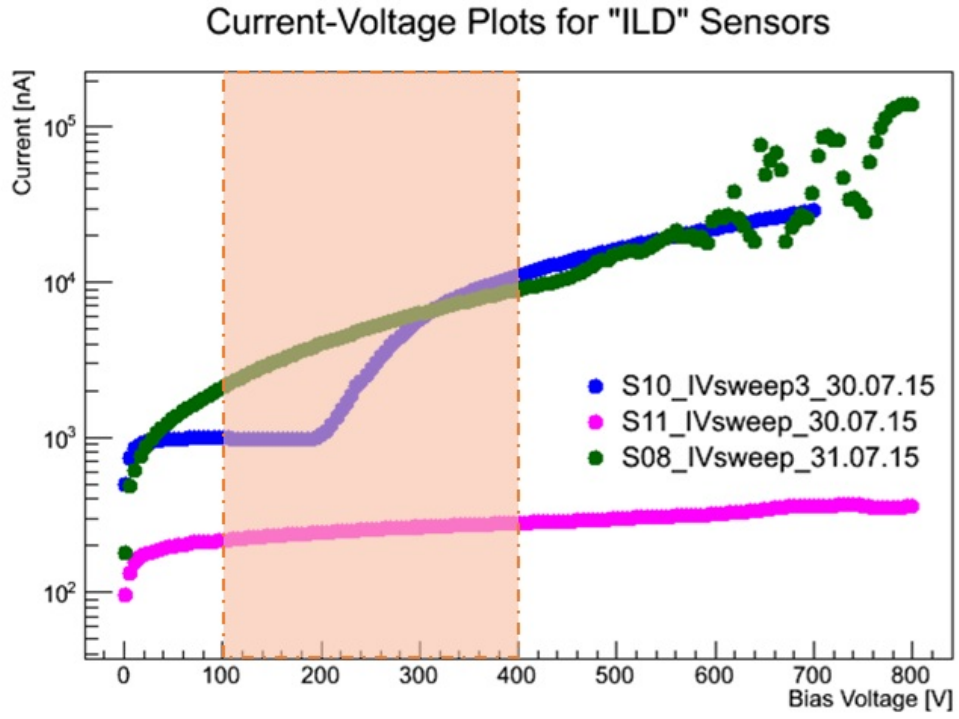


Figure 12: Plot of Current versus bias voltage for the silicon sensors. The shaded region is the typical operating voltage.

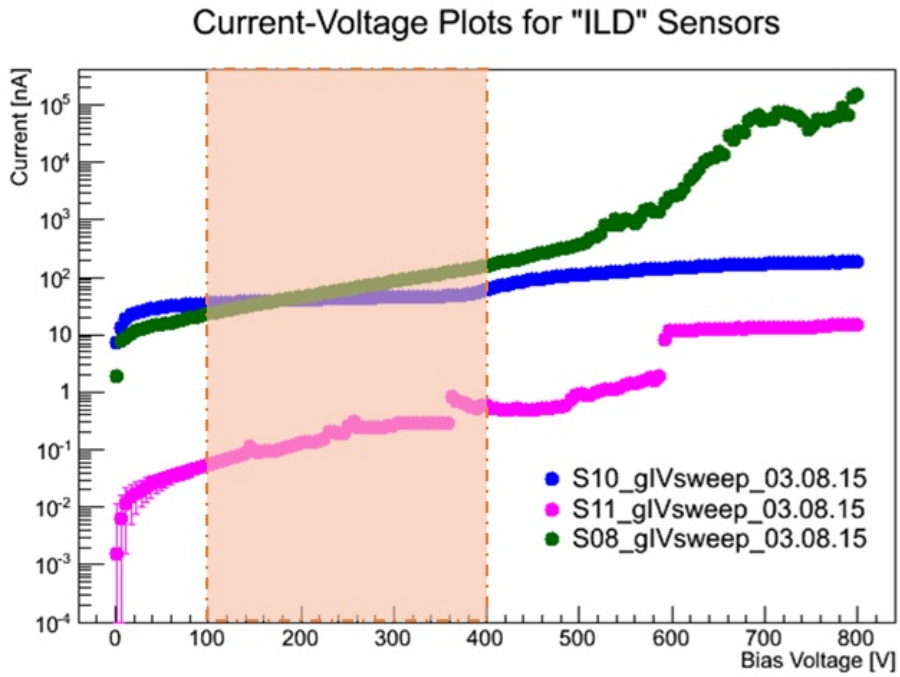


Figure 13: Circuit diagram for the gIV measurement. The shaded region shows the typical operating voltage

6.3 Depletion Voltages from CV Curves

Figure 14 shows the plot of one over the square of the capacitance as a function of the applied voltage.

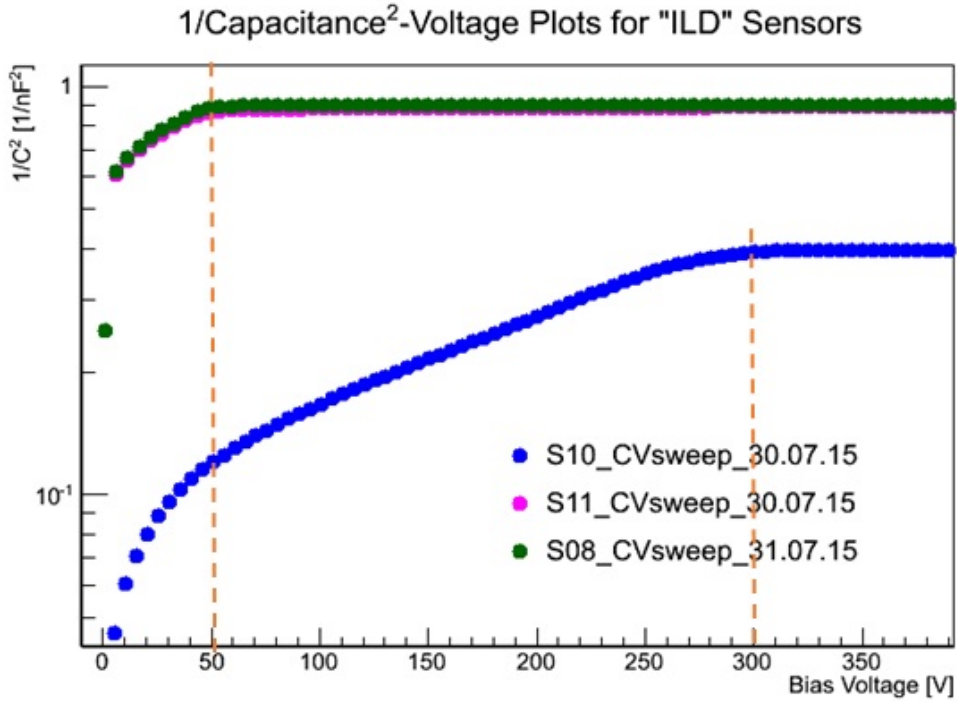


Figure 14: Circuit diagram for the CV measurement. The dashed lines show the depletion voltages of the two types of sensor

In figure 14, the orange line shows the depletion voltage for each sensor. The CMS sensor depletes at around 300V, and the SILC sensors deplete at around 50V. Due to the relatively low value at which the SILC sensors deplete, when operating the sensors with electronic readout it may be necessary to over-deplete the sensors by applying a higher bias voltage. This is because silicon electronics are fast and require fast collection times. If the electric field at which the liberated information carriers is low, then the collection of charges will be slow which causes large uncertainties in track reconstruction .

6.4 Bias Resistances

Figure 15 shows the plot that is the result of the bias resistance measurements carried out in the way described in section 5.3.1. Four resistors from the CMS sensor have measured resistance values, and a spread thereof, that are consistent with those measured by the CMS collaboration of $2.0 \pm 0.6 \text{ M}\Omega$ [15, p130] but the lines do not intersect with the origin.

However, when the same set-up was used to probe the bias resistances of the SILC bias resistors, the curves that are displayed in figure 16 were obtained, which are more similar to the IV trend of a diode rather than a resistor. The set-up was then varied, and the same experiment was repeated to try and determine the cause of the non-ohmic resistance curve. Figure 17 shows three different set-ups: The original in blue (with a depletion voltage applied and a ground probe) labelled w/GP&DV, a set-up without the ground probe but with a depletion voltage in pink labelled w/DV, and a set-up with no ground probe or depletion voltage in green.

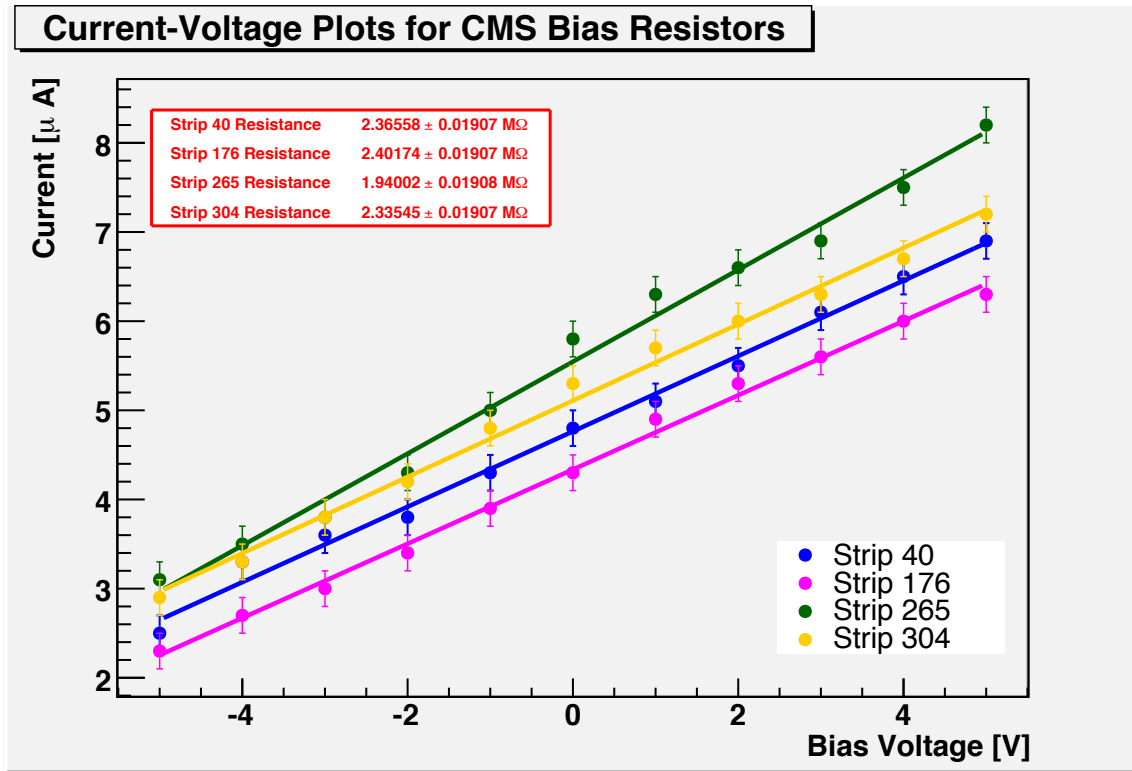


Figure 15: Plot of current versus low voltage for the CMS sensor.

Figure 16: Plot of current versus low voltage for the SILC08 sensor with a ground probe in the set-up.

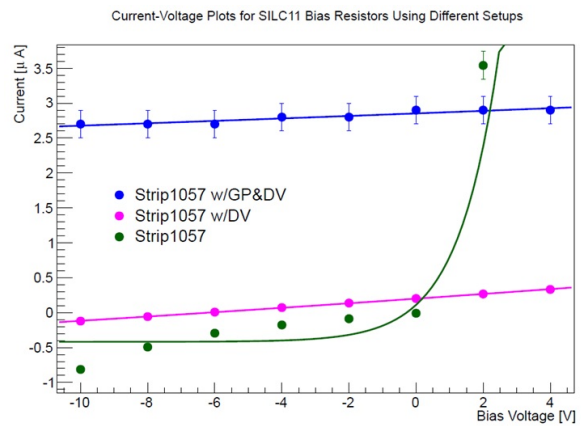
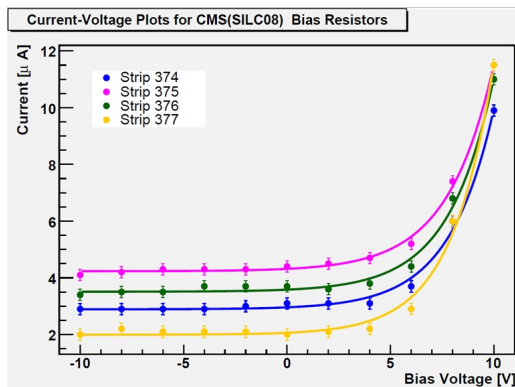


Figure 17: Plot of current versus low voltage for different experimental set-ups.

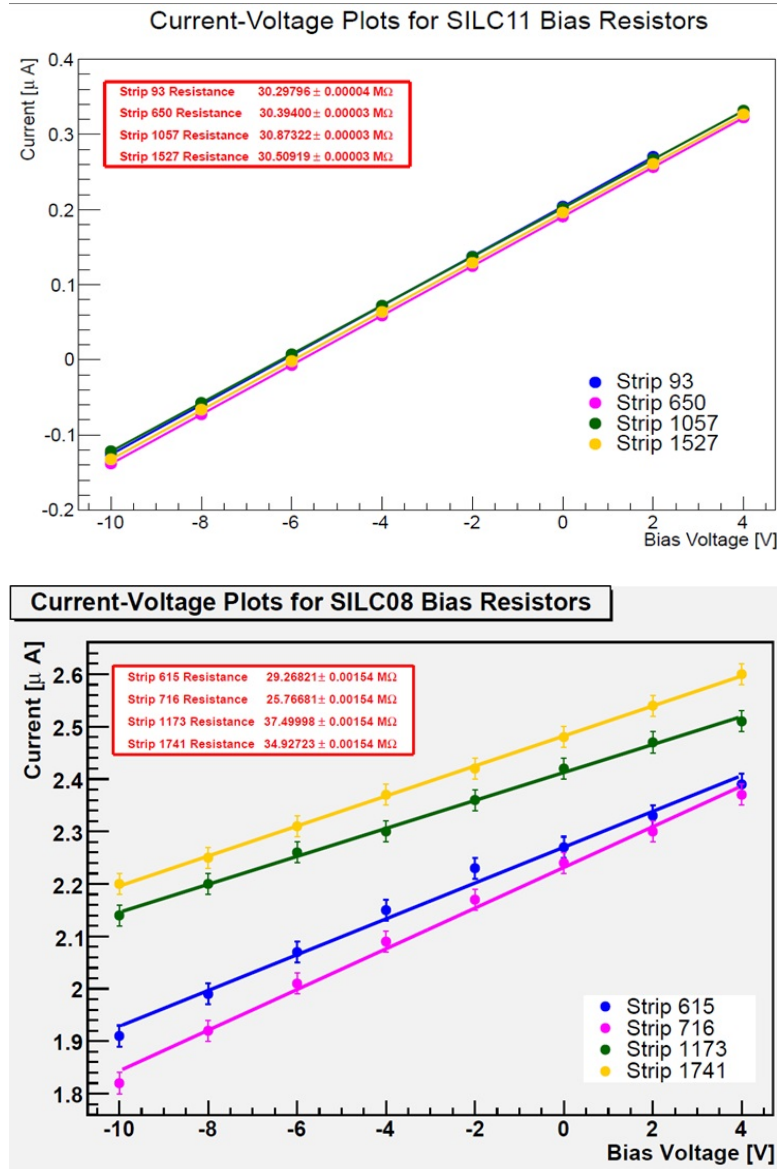


Figure 18: Plot of current versus low voltage for the SILC sensors.

According to figure 17, the set-up that obtains the linear correlation that is closest to the origin is the line in pink, and hence the set-up without the ground probe will be used to measure the resistance of the sensors.

Figure 18 shows the plots that are the result of using the corrected set-up. For both sensors the resistance seems to be about $30M\Omega$ but the spreads vary. For a true account of the average bias resistance and the variance, more statistics are needed. This data is a conclusion from 4 strips out of the 1792 strips on the sensors, so this only hints at the true resistance pattern of the sensors.

7 Conclusion and Outlook

Silicon sensors that can fulfil the stringent requirements of $10\mu m$ spacial resolution and can be used for a Silicon external tracker for the LPTPC have been tested for this study in order to fully understand their capabilities. The results of the sensor characteristics are only the first

step to understanding the capabilities of the sensors.

- The IV curves obtained show that the breakdown voltage of the silicon sensors is above 800V.
- The current leakage from SILC08 and SILC11 is low compared to the current in the bias ring at the voltages the sensors should be operated at (100-400V).
- The CV observations conducted show that the depletion voltage of the SILC Sensors is around 50V and confirm the IV curves that show that the sensors do not break down up to 700V.
- The Bias Resistance measurements of SILC11 and SILC08 are about $30\text{M}\Omega$, with a larger variation in SILC08 than in SILC11. The variation in these values, however, is in line with measurements of these characteristics by previous independent studies.

However, there are still tasks to be completed. To get a good idea how good the strips are at containing charge, and how much current leaks from one strip to another, the inter-strip characteristics of the sensors should be explored. Since the probe-station that these tests were done on were manual, more statistics on the sensors would be very beneficial. For example, with an automated process, the bias resistance of a larger proportion of the 1790 strips could be plotted against strip number to see if there were any trends in the resistances of the sensors or any large patches of sensors that have abnormal traits. After these measurements the next step is to connect the strips to a signal readout and see if the sensors can perform to the precision that is required and understand any processes that prevent this from happening.

8 References

- [1] T. Behnke, J. E. Brau, B. Foster, J. Fuster, M. Harrison, J. M. Paterson, M. Peskin, M. Stanitzki, N. Walker, and H. Yamamoto, “The International Linear Collider Technical Design Report - Volume 1: Executive Summary,” p. 9, 2013.
- [2] T. Behnke, F. Müller, A. Münnich, and K. Zenker, “GEM Module Design for the ILD TPC,” *JINST*, vol. 8, p. C10010, 2013.
- [3] P. Schade, *Development and construction of a large TPC prototype for the ILC and study of tau polarisation in stau decays with the ILD detector*. PhD thesis, Hamburg U., 2009.
- [4] H. Abramowicz *et al.*, “The International Linear Collider Technical Design Report - Volume 4: Detectors,” 2013.
- [5] R. L. Gluckstern, “Uncertainties in track momentum and direction, due to multiple scattering and measurement errors,” *Nucl. Instrum. Meth.*, vol. 24, pp. 381–389, 1963.
- [6] D. Tsionou, “Simulation studies for a silicon telescope in test beam area T24/1 accompanying the LCTPC prototype,” 2015. Internal Note.
- [7] H. Spieler, *Semiconductor Detector Systems*. Oxford Science Publications, Oxford University Press, 7th ed., 2005.
- [8] M. Krammer, “Silicon detectors part 2.” XI ICFA School on Instrumentation Lecture Series.
- [9] M. Krammer, “Silicon detectors part 3.” XI ICFA School on Instrumentation Lecture Series.
- [10] D. C. Arogancia *et al.*, “Study in a beam test of the resolution of a Micromegas TPC with standard readout pads,” *Nucl. Instrum. Meth.*, vol. A602, pp. 403–414, 2009.
- [11] P. Horowitz and H. Winfield, *The Art of Electronics*. Cambridge University Press, 2 ed., 1989.
- [12] S. Hänsel, *Studies for the Silicon Tracking System of the International Large Detector at the International Linear Collider*. PhD thesis, Vienna, Tech. U., 2011-02-14.
- [13] R. Barlow, *Statistics A Guide to the Use of Statistical Methods in the Physical Sciences*. 6 ed., 1999.
- [14] F. Hartmann, *Evolution of Silicon Sensor Technology in Particle Physics*, vol. 231. 2009.
- [15] C. Collaboration, *CMS, tracker technical design report*. 1998.

9 Acknowledgements

I would like to thank my supervisor Dr Dimitra Tsionou for her invaluable help, advice and support throughout my time at DESY. To Dr Annika Vauth and Ralf Dernier who helped me with my coding and presentations, I also offer my thanks, and a special thank you goes to Dr’s Doris Eckstein, Ingrid Maria-Gregor and Marcel Stanitzki who gave me valuable pointers and papers whilst my supervisor was away. I would like to thank Aliakbar Ebrahimi for his help with the laboratory set-up. Lastly I would like to thank all the other members of the FLC TPC group for making my 8 weeks on this project enjoyable.